International Journal of
INTELLIGENT SYSTEMS AND APPLICATIONS IN ENGINEERING
ISSN:2147-6799 www.ijisae.org Original Research Paper

UWB Microstrip Fed 4-Element MIMO Antenna For 5G Applications

B. Santhikiran[1]*, Dr. T. Kavitha[2]

Submitted: 26/04/2023 **Revised**: 27/06/2023 **Accepted**: 06/07/2023

Abstract: The work in this article is used for the design and testing of a low-density microstrip feed line that is connected to a Multiple-Input-Multiple-Output antenna incorporated with the 5G applications on Wireless LAN (5.152 -5. 80GHz) and IEEEE INSAT / super Extended C band (6.7-7.1 GHz) and IEEEE INSAT / Extended C band (6.70-7.10 GHz). The inclusion of planar form is that the tiny structure can be used for many applications along with a wide range of active bandwidth, excellent efficiency, and improved radiation efficiency. A compact redesigned antenna in the form of two L-shaped feeds with H centered slot to the surface of the rectangular patch is utilized. The 4- element structure is designed by arranging the model of a monopole antenna in a rotating orthogonal way. A rectangular patch connects the ground plane under a 4-element structure, the isolation separation levels to be > 20 dB above the interested band. The 4-component MIMO antenna has a minimum dimension of 80*80*1.6mm3 and stretched bandwidth (25.7-35.5) GHz, maximum 10dB gain, and 85% minimal efficiency in all interested bands. The implementation of the suggested antenna is performed with the addition of polyimide substrate and tested experimentally, with satisfactory scattering and transmission properties.

Keywords— *MIMO Antenna, the Ultra wideband, defected microstrip fed MIMO diversity.*

1. Introduction

With the increasing rise of high data rates, optical performance, delays, the price, and the requirement for a better channel network of communication capacity, For large-scale coverage, low 5G NR sub-6 GHz frequencies are currently being used [1, 2, 3]. As a result, the new frequency band on 5G New WLAN Radio and INSAT are optimized for a wide range of applications requiring multi-gigabit data rates per second [4,5]. The frequency of 5G wave applications has been increased in the US(28.0 GHz, 37.0 GHz, and 39.0 GHz), Japan(27.5.0–28.8.0 GHz), and China(24.25–27.50 GHz, 37.0–43.50 GHz) and Korea (28.0 GHz) [6].

Ultra Wide Band (UWB) is an emerging wireless communication technology that has been used in recent years. This meets the needs of modern communication systems in both broad bandwidth and high profitability.

In wireless communication, however, the deterioration of multiple paths has a significant impact on UWB technology. The usage of the MIMO Antenna, which increases the power of wireless communication networks, is one of the limitations.

For MIMO antennas, selecting antennas from several available antennas during the generation of an interconnected ground plane is a tough task [7-8]. Decoupling structures [9], have been used to increase antenna separation in MIMO systems: Defected Ground Structure [10], Electronic Band Gap [11-12], and Split Ring Resonator [13]. Wide bandwidth is another necessity of UWB technology, which is impossible to acquire with standard patch antennas due to their low bandwidth. Various techniques, such as a slotted microstrip-fed [14], 4 elements that include a rectangular angle and corners [15], a single-pole antenna with Split Ring Resonator, and the ring-shaped globe [17] are the types of antenna used to acquire the aforementioned bandwidth. The designing of MIMO antenna with the same type of antenna is advisable to increase the actual use of the antennas [18].

The use of 2 MIMO antennas on a single mm-wave [19] and dual [20] frequency bands is stated incorporated with [19] connected profile and [20] with a different ground structure. Because two dipole structures are not large enough to cater to a large number of available customers and hence four port-operated antennas are required. In the mm-wave single states [21, 22], dual [23, 24], and wide-band [25, 26, 27], four-port antennas are stated and all of these exclude [27] the connected ground plane.The proposed antennas [23] and antennas in [24] consider a dual-frequency band with access to the mm-wave application band but do not include the entire 5G band, so the four-port MIMO is preferred. Although the stated antennas in [25, 26, 27] can availof the 5G spectrum, the dimensions of the recommended antennas in [25, 26] are greater than the above-stated one. Nevertheless, the stated antenna in [27] was small and covers a wide range of mm 5G waves, however, it has a different base, As a result, it's not ideal for real-time applications

[1]*Department of ECE, Vel Tech Rangarajan Dr. Sagunthala R&D Institute of Science and Technology, Avadi, Chennai, Tamil Nadu, bsk.aliet@gmail.com.*
[2]*drkavitha@veltech.edu.in.*

For wideband mm-wave applications, a small antenna with four vertical ports (24 *24 mm2) with a slot that is elliptical in the center, a coplanar feed that has been modified, and a lower plane section have been utilized. The increase in the bandwidth is obtained via adjusting with extreme caution, the design of the ground plane and the elliptical slot in the center. The suggested 4-Element antenna works in a range of 25.7 to 35.5 GHz and has a separation of more than 20 dB between ports. MIMO diversity and satisfying diversity are added to the integrated profile. HFSS is used to simulate and test a design.

The proposed antenna creates radiation patterns in Omnidirectional with a gain of 10.2db,85% low efficiency, and also it gives ECC <0.003, DG>15db in a whole range of spectrum frequency based on the results the antenna is simulated and observed on HFSS toll and Vector Network Analyzer. The suggested work is applicable for 5G applications.

The rest of the article is organized accordingly: The geometry of the antenna to be designed is depicted in section II. The element used for the MIMO antenna is explained in section III. The designing and evaluation of four elements of MIMO are elucidated in section IV. Various diverse MIMO schemes are deliberately explained in section V. The radiation patterns and fabrication steps are explained in section VI.

2. Geometry of Antenna Design

This section presents the geometrical features of the antenna to be designed. The antenna with a monopole, folded gap, and short edges are shown in Fig.1. The delivery of this monopole antenna comes from the coplanar waveguide (CPW). The following figures show the basic formulas in the design of monopole antennas for CPW feeds.

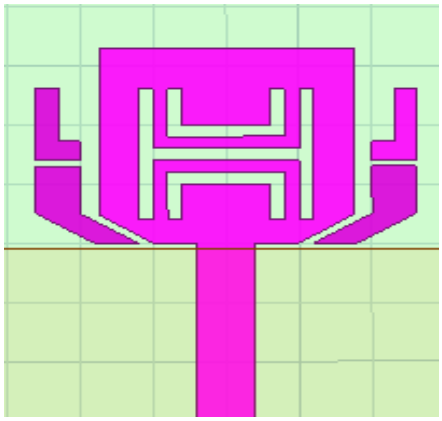

Fig:1 The Proposed Antenna in Single pole.

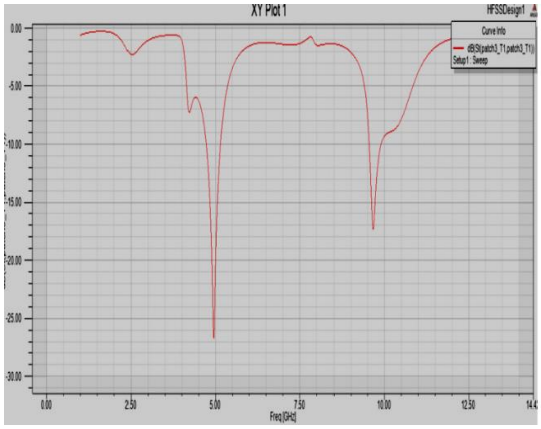

Fig: 2 S11 plot of single-pole antenna**.**

CPW is determined by the following equation:

$$Ereff=(Err+1)/2\{\tanh[0.775\ln(h/G)+1.75]+Kg/h\times[0.004-0.7k+0.01(1-0.1Er)(0.25+k)]\} \quad (1)$$

where, $k = W/W + 2G$ (2)

W= Center conductor width,

h = Substrate thickness,

G =There is a gap space between the conductor and the ground.

The formula for calculating the ratio of first order elliptic integral and its complement is

$$Z\ 0CPW = 20\pi/\sqrt{Ereff}\ K'(k)/K(k) \quad (3)$$

$$K'(k)/K(k) = [\pi/\ln(2(1+\sqrt{k})/(1-\sqrt{k}))]$$

If $0 < k < 0.707$

$$= [\ln(2(1+\sqrt{k})/(1-\sqrt{k}))/\pi] \text{ If } 0.707 < k < 1 \quad (4)$$

From equation 4, the theoretical values are of Ereff = 2.809, Z0CPW ~= 48Ω for the dimensions of W = 2.0mm, h =1.60mm, G = 0.30mm and r = 4.40mm. Ultra-wideband has achieved it and ranges are 2.4GHz to 18.6GHz with a bandwidth of 15.6GHz. H-slots near dual slots are equipped with rectangular radiation features to achieve dual-band notch structures. The parameters taken in equation (5) are used for the determination of maximum H sizeand the U-shaped stubs are set in the frequency of the middle notch band.

$$Ls = \lambda g/4 \quad (5)$$

$\lambda g=\lambda o\backslash sqrt(\varepsilon)r$

λg = guided in wavelength $\lambda o = c0$

fr = wavelength in free space,

fr =center frequency of notch band

c0 = light of velocity

εr = dielectric constant

Figure 1 shows a statistical view of a perforated

monopole radio wave and an H-shaped monopole system that receives H-shaped slots, This receiving wire is made as a prototype on the polyimide substrate with a diameter of 37*40*1.6 mm3. This proposed receiving monopole antenna has a transmission capacity from, 2.2 GHz - to 18.4 GHz, and 3.6 GHz (WiMAX) and 8.3 GHz (military and radar) scores, as shown in Fig.2, In this way, the intended and repeated acquisitions should be the same.

In addition, the impact of the redesigned CPW feed is evaluated with the U-shapedslots, and the display coefficient's performance is tested. In fig.1 the two tiny patches with a radius of 1.5 mm are placed beside the given patch.

An H slot is designed to increase the performance of the given antenna and also estimates the amount of correlation in different space sizes. It also improves the 10 dB impedance bandwidth performance and displays coefficient levels, especially for low-frequency bands, when operating from 25.7 to 35.5GHz.

3. 4- Element Mimo Antenna

To construct the 4-element antenna the single antenna elements are arranged in an orthogonal rotation with their ground, as shown in Fig. 3. The minimum distance between MIMO elements is maintained by k; this perpetuates the mitigation of compounding effects and thus ensures spatial diversity performance in it. In addition, the proposed design avoids obstructions of similar members, by providing distance between elements of the same members in order to cut the connector space.

HFSS software is used to design the MIMO four-element antenna. Excess current distribution at various frequencies (3.655 GHz, 5.8 GHz, 10.145 GHz, 20.145 GHz, and 30.205 GHz) is investigated by regenerating one hole while leaving the others under the investigation ofa load of 50 X, as shown in Figures.5-9, It shows that the antenna excitement in various operating waves reduces leakage, which is manifested due to local variability and a different floor profile. In addition, the distribution parameters can be used to justify the power distributed at least from one pole to another, when the gap between the holes is greater than 20 dB, as seen in Fig.7.

Despite the antenna's great performance (as shown in Fig. 4), its practical application is limited due to the soil profile. However, it requires at least one common method that connects all sub-planes to be embedded in a standard printed circuit board (PCB) structure without compromising the performance of individual ports.

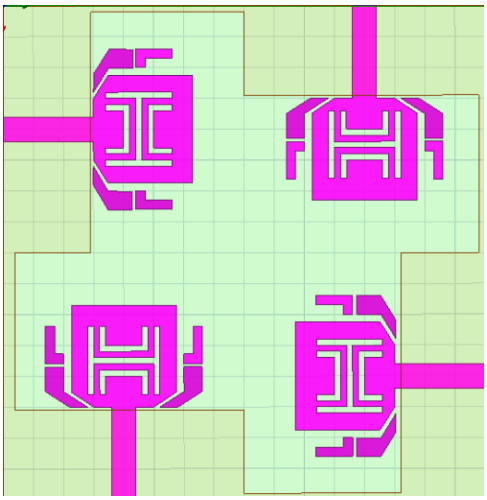

Fig.3 Proposed 4 Element Orthogonal Antenna**.**

The ECC values of the proposed model with an orthogonal 4-element MIMO antenna are approximately 0.019. For example, if the ECC value of the antenna is approximately 0.05, then the practical application of the antenna is limited; meanwhile, when the converted ECC value is less than or equal to 0.03, then it is deemed as the best antenna. When the value of ECC is reduced, segregation also suffers. We have chosen this shape instead of because we want the ECC value to be less than 0.03. With our proposed antenna, the ECC value obtained is approximately 0.019.

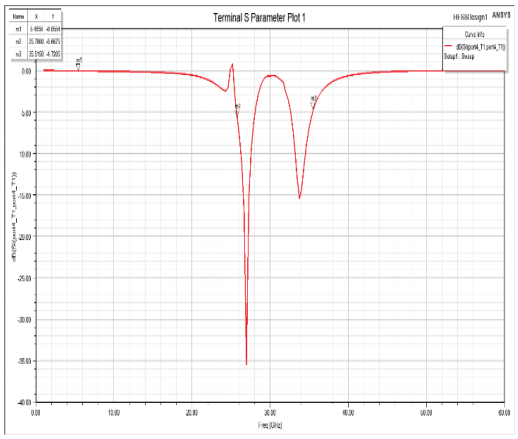

Fig.4 S11 Plot of Proposed 4 Elements Orthogonal Antenna.

As illustrated in Figures 5–9, the a fore mentioned power distribution is evaluated by varying frequencies (3.655 GHz, 5.8 GHz, 10.145 GHz, 20.145 GHz, and 30.205 GHz)to have a better understanding of the MIMO series' performance incorporated with the correlation between the items The power integration in the operational bandwidth is quite low, even with the addition of an L-shaped patch that forms a connected ground structure. This depicts the separation among the MIMO objects.From Fig. 4, the upper and lower constraints of our antenna design generate an Excellent 20 dB transmission frames and width passing bandwidth (79.35 percent) from 25.7 to 35.5GHz.

4. Design and Evaluation of 4-Element Antenna

The top and bottom views of the antenna designed in the polyimide substrate are illustrated in figures 11 and 12.

The coefficient used for the reflection of our designed antenna outcomes is depicted in figures 13 to 15. At frequencies between 25.7 and 35.5GHz, the predicted coefficient value is better as compared to 10 dB and nearly identical to the measured result. Although the results are within the capabilities of 5G applications, the modest differences in performance are attributable to network connectivity and performance limitations. MIMO antenna applications for chosen frequency bands are also provided.

The setting of the radiation pattern in the anechoic chamber with the activation of one object at a time is depicted in figure 16. However, the same load is shared by the other three elements in the MIMO system.

TABLE 1: COMPARISON OF H & F ANTENNAS

PARAMETERS	H	F
SIZE	80*80*1.6mm3	30*26*106mm3
Impedance Bandwidth	S11<10db (2.4ghz-18ghz)	S11<-10db(3.2ghz-3.8ghz) And S12<20db(5.7ghz-6.8ghz)
ECC	<0.19	<0.03
Directivity Gain	~10	9.8
Peak Gain	5.9	5.08
Radiation Efficiency	82%	80%
Mutual Coupling	<-20db	<-20db
Isolation	Split Ring Resonator	Elliptical Slot And Rectangular Parasitic Strips Contribution To High Isolation
FEEDING	Micro-strip	CW
SUBTRATE	Polyimide	Polyimide

5. Mimodiversity Schemes

To expand the actual implementation, the designed 4-element MIMO antenna performsa variance analysis based on the DG and ECC. In the MIMO 4-element flexible antenna, the operating conditions of the MIMO vary with the ECC and estimated the value using equation (a) [30].

$$ECC = \frac{\left|(S11*S12)+(S21*S22)\right|}{\left(1-\left|S11\right|^2-\left|S21\right|^2\right)\left(1-\left|S22\right|^2-\left|S12\right|^2\right)} \quad \text{(a)}$$

1. SURFACE CURRENT DISTRIBUTION:

The investigation of current overhead at the 3.6GHz and 8.3GHz notch, as well as the 5.5GHz and 10 GHz performance band of the proposed four-dimensional antenna is performed.

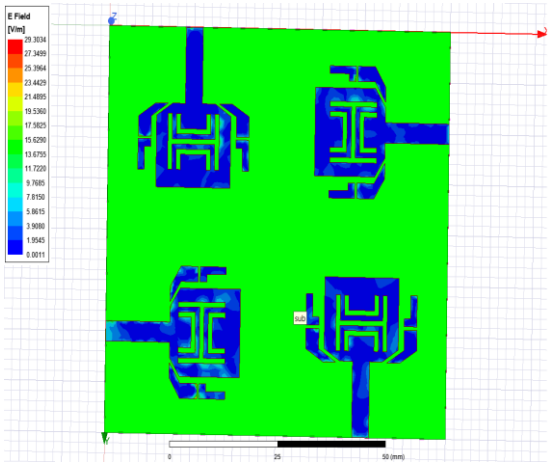

Fig.5: E-Field at 3.655GHz

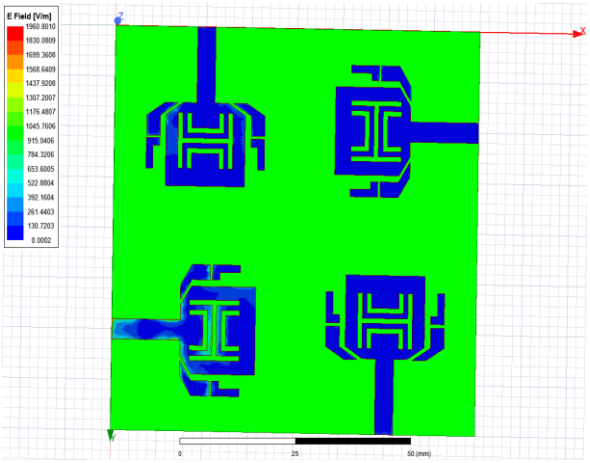

Fig.6 E-Field at 5.8Ghz

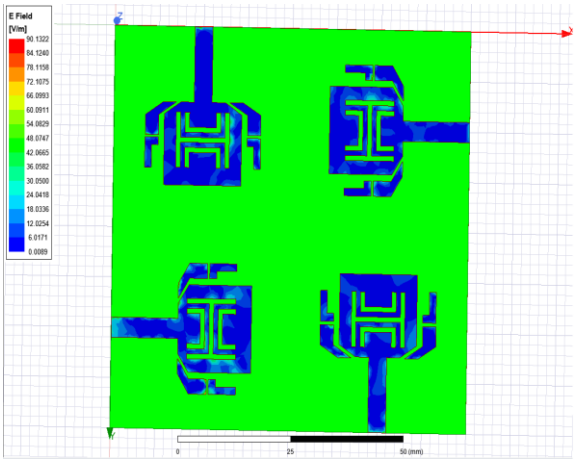

Fig.7 E-Field at 10.145Ghz

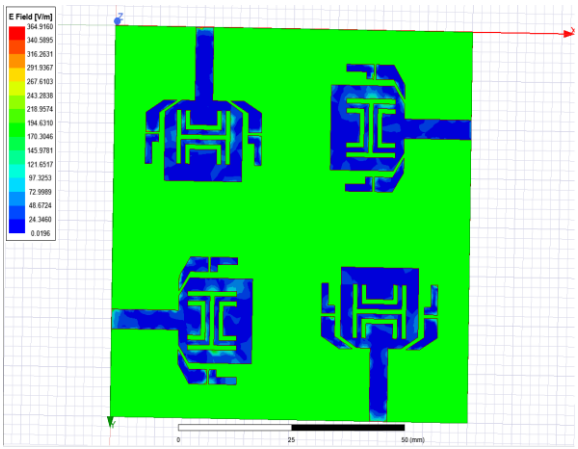

Fig.8 E-Field at 20.145Ghz

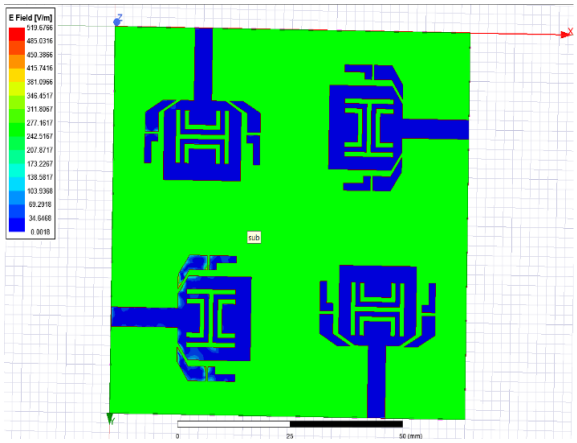

Fig.9 E-Field at 30.205Ghz

Figures [17-22] show the two-dimensional radiation designs in the polar directions of the two parts of the MIMO radio cable at 10 GHz and 5.8 GHz frequencies among various planes, such as the x, y, and z planes. The x-plane, or receiving plane, is used by two MIMO components that act as the receive cables. Finally, co-division occurs by Gain-phi value and co-division occurs by Gain-theta value are estimated and plotted.

2. ENVELOP CORRELATION COEFFICIENT (ECC):

The differences between the 2 MIMO radio cable components are considered. The integrated connection of the MIMO radio port1 & port2 can produce a radiant design. The envelope co-relation coefficient of any Multi-input Multi-output antenna should be less than 0.5 to indicate good variability. Both the measured and experimental ECC ratings exceed 0.02 of the entire 5G range switching indices.

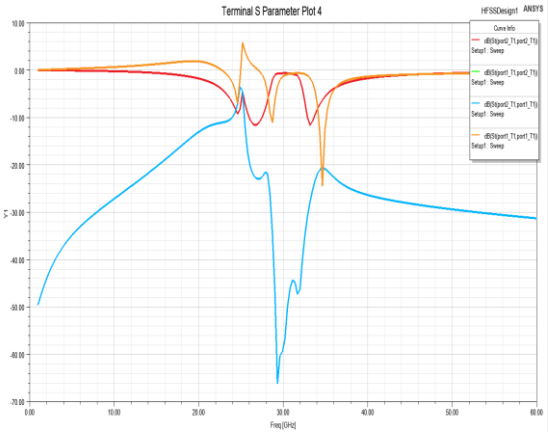

Fig.10: S parameters of 4Element Orthogonal MIMO Antenna.

3. DIVERSITY GAIN (DG):

DG is measured by the antenna parameters, which can be defined as the reduction in transmission power after the introduction of the diversity scheme and can be expressed as,

$$DG = 10\sqrt{(1 - ECC)^2} \qquad \text{(b)}$$

6. Fabrication Results and Radiation Patterns

Figures [17-22] Show the calculated gain as well as the efficiency of the designed antennas. The proposed mm-wave antenna's gain is >5dB and Efficiency is85 percent in the necessary band.

Based on operating parameters such as used material, port number, connected ground profile, location, bandwidth performance, profitability, efficiency, isolation, and ECC, the proposed MIMO antenna for the stated wave is compared to other antennas. The proposed states are integrated and give larger bandwidth, sufficient profitability, and efficiency over the stipulated bandwidth, with strong separation from the lower ECC and listed in table 1.

The difference between the proposed MIMO small Antenna small mm-wave 4 and other pre-designed radiators are stated below:

- Focuses on the width of the sub-mm-wave frequency.
- Construction is small, measuring only 24* 24 mm2.
- Even with a connected ground profile, there is a high degree of isolation between ports.
- Increase radiation efficiency by using a polyimide substrate.
- Designing is made easy with the factors of orderliness and simplicity.

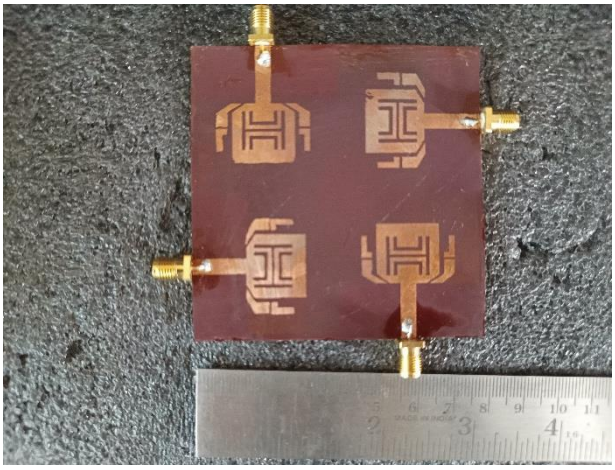

Fig.11 Fabricated Antenna's Top view

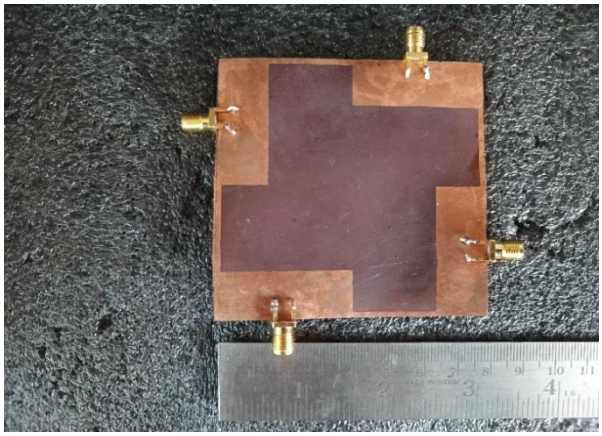

Fig.12 Fabricated Antenna's Bottom view

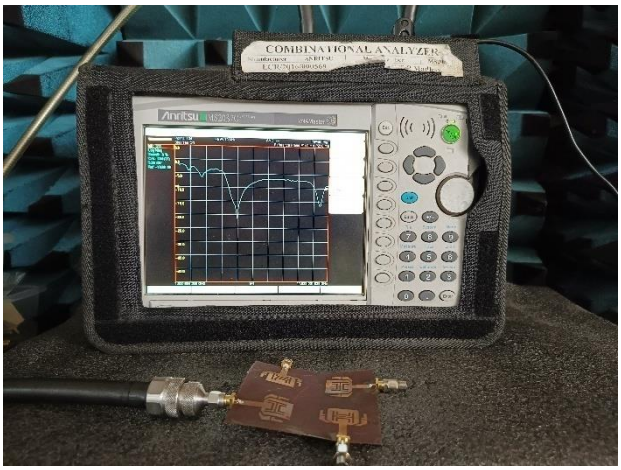

Fig.13 S11 Plot of Fabricated Antenna From VNA

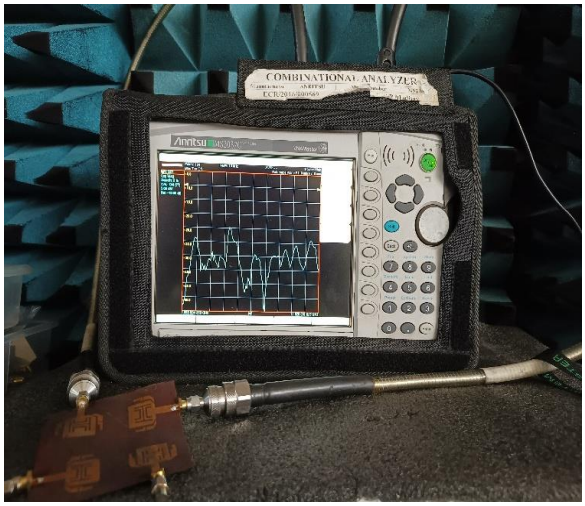

Fig.14 VNA results of S12/S21 Plot of Fabricated Antenna

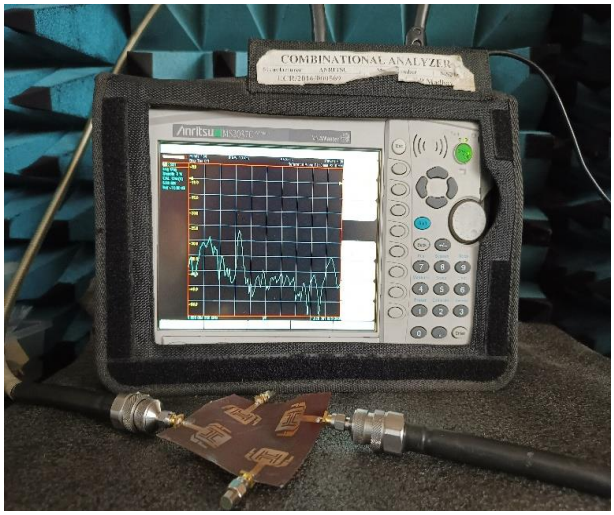

Fig.15 VNA results of S13 Plot of Fabricated Antenna

Fig.16 VNA results of VSWR Plot of Fabricated Antenna

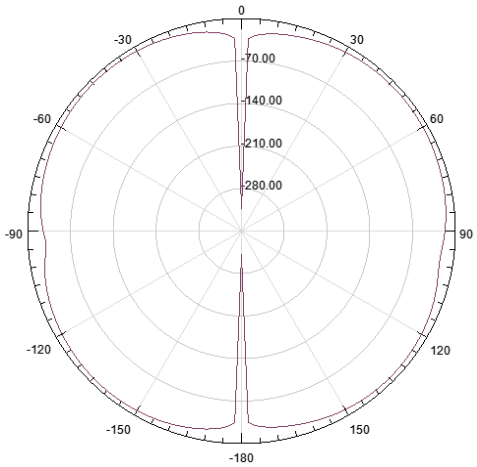

Fig.17 X plane radiation pattern at 5.8GHz

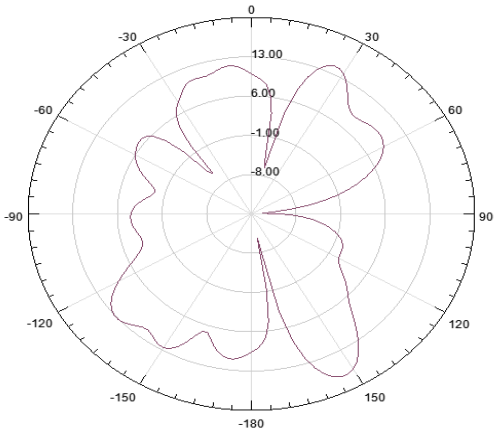

Fig.18 X plane radiation pattern at 10GHz

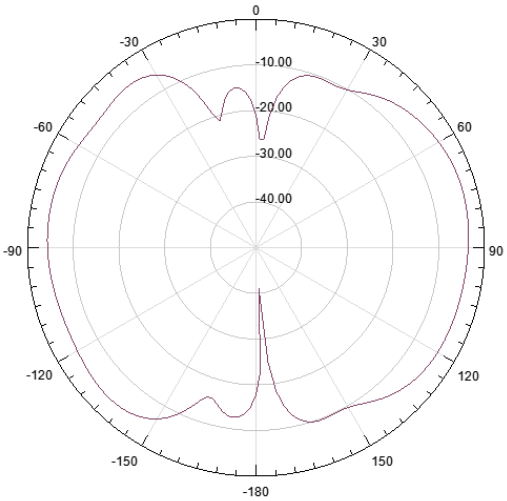

Fig.19 Y plane radiation pattern at 5.8GHz

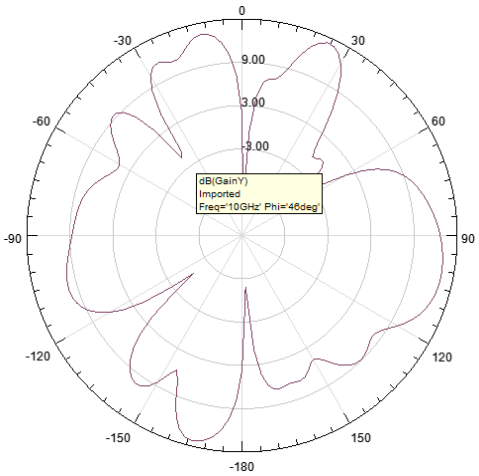

Fig.20 Y plane radiation pattern at 10GHz

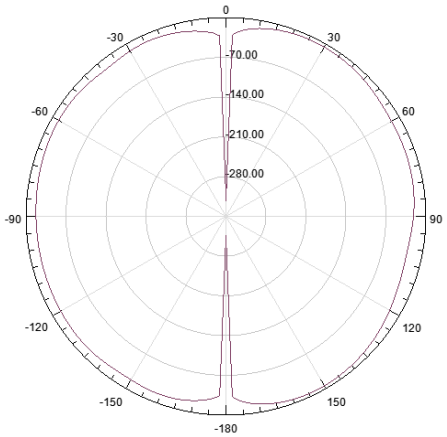

Fig.21 Z plane radiation pattern at 5.8GHz

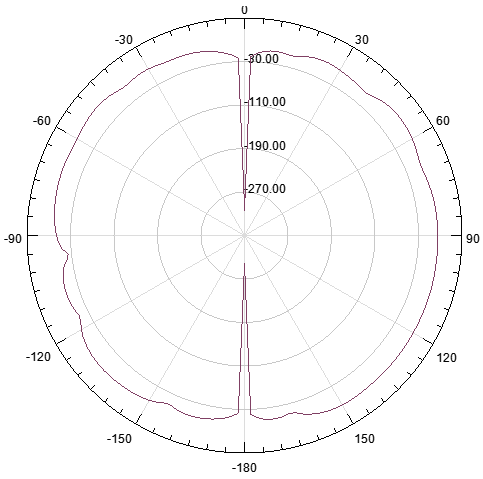

Fig.22 Z plane radiation pattern at 10GHz

7. Conclusion

In this article, a 5G system with an orthogonal 4 element MIMO antenna (80*80*1.6mm3) with an integrated ground structure of polyimide has been proposed. The designed antenna is analyzed with performance-based performance parameters, augmented antenna design, and also made detailed MIMO diversity analyses. Maximum bandwidth can be obtained with the inclusion ofan H

slotted L patched antenna. 85% of bandwidth along with 20db systematic separation has been acquired. Moreover, the radiation patterns were applied in all directions with the Envelop Correlation Coefficient valueof0.02, and DG > 10.2 dB, medium gain of > 5.680dB and Efficiency of 85.0. further, the strong diversity has been achieved by our proposed antenna with a low ECC of 0.019.Furthermore, the stability of antenna gain has been enhanced along with the directional radiation patterns, and impedance bandwidth with dual notches. This shows that the proposed antenna can be used for many 5G MIMO applications with adequate antenna performances.

8. Compliance with Ethical Standards

Conflict of interest

The authors declare that they have no conflict of interest.

Human and Animal Rights

This article does not contain any studies with human or animal subjects performed by any of the authors.

Informed Consent

Informed consent does not apply as this was a retrospective review with no identifying patient information.

Funding: Not applicable

Conflicts of interest Statement: Not applicable

Consent to participate: Not applicable

Consent for publication: Not applicable

Availability of data and material:

Data sharing is not applicable to this article as no new data were created or analyzed in this study.

Code availability: Not applicable

References

[1] T.S. Rappaport, S.Sun, R.Mayzus,H.Zhao, Y.Azar,K.Wang,G.N.Wong,J.K.Schulz,M.Samimi,F. Gutierrez,Millimeterwavemobilecommunicationsfor5 Gcellular:Itwillwork,IEEEAccess1(2013)335–349.

[2] R.G.Vaughan,J.B.Andersen,Antennadiversityinmobil ecommunications,IEEETrans.Veh.Technol.36(4)(198 7)149–172.

[3] Z.Pi,F.Khan,Anintroductiontomillimeter-wavemobilebroadband systems,IEEECommun.Mag.49(6) (2011) 101–107.

[4] S. Kim, E. Visotsky, P. Moorut, K. Bechta, A. Ghosh, and C.Dietrich,''Coexistenceof5Gwiththeincumbentsinthe 28and70GHzbands,"IEEEJ.Sel.AreasCommun.,vol.35 ,no.6,pp.

[5] 1254_1268,Jun.2017.

[6] J.-H.Lee,J.-S.Choi,andS.-C.Kim,''Cellcoverageanalysisof28 GHz millimeter wave in urban microcell environment using 3-D ray tracing, ''IEEE Trans. Antennas Propag., vol. 66, no. 3,pp.1479_1487,Mar.2018.

[7] A.Desai,T.Upadhyaya,R.Patel,Compactwidebandtrans parent antenna for 5G communication systems, MicrowOptTechnolLett61(3)(2019)781–786.

[8] R. Krishnamoorthy, A. Desai, R. Patel, A. Grover, 4 ElementcompacttriplebandMIMOantennaforsub-6GHz5Gwirelessapplications,WirelessNetw.(2021)1–13.

[9] M.S. Sharawi, Current misuses and future prospects for printedmultiple-input,multiple-outputantennasystems[wirelesscorner],IEEEAntennas Propag.Mag. 59(2)(2017)162–170.

[10] IrshadKhan, Muhammad,Muhammad Irfan Khattak, SaeedUr Rahman, Abdul Baseer Qazi, Ahmad Abdeltawab Telba,and Abdelrazik Sebak. ''Design and investigation of modernUWB-MIMOantennawithoptimizedisolation."

[11] Micromachines11,no.4(2020):432.

[12] J. Banerjee, A. Karmakar, R. Ghatak, D.R. Poddar, CompactCPW-fedUWBMIMOantennawithanovelmodifiedMinkowski fractal defected ground structure (DGS) for highisolationandtripleband-notchcharacteristic,Journalofelectromagnetic Waves and Applications 31 (15) (2017) 1550–1565.

[13] I. Nadeem, D.-Y. Choi, Study on mutual coupling reductiontechniqueforMIMOantennas,IEEEAccess7(2019)563–586.

[14] N.Kumar,K.UshaKiran, Meander-line electromagneticbandgapstructureforUWBMIMOantennamutualcouplingreduction in E-plane, AEU-International Journal of ElectronicsandCommunications127(2020)153423,https://doi.org/10.1016/j.aeue.2020.153423.

[15] A.Ramachandran,S.Mathew,V.Rajan,V.Kesavath,Acompacttribandquad-elementMIMOantennausingSRRringforhighisolation,IEEEAntennasWirel.Propag.Lett.16(2017)1409–1412.

[16] M. Sonkki, D. Pfeil, V. Hovinen, K.R. Dandekar, WidebandPlanar Four-Element Linear Antenna Array, IEEE AntennasWirel.Propag.Lett.13(2014)1663–1666.

[17] A. MoradiKordalivand, T.A. Rahman, M. Khalily, CommonElementsWidebandMIMOAntennaSystemforWiFi/LTEAccessPoint Applications, IEEE Antennas Wirel. Propag. Lett.13(2014)1601–1604.

[18] H.Wang,L.Liu,Z.Zhang,Y.Li,Z.Feng,AWidebandCompact WLAN/WiMAX MIMO Antenna Based on DipoleWith V-shaped Ground Branch, IEEE Trans. Antennas Propag.63(5)(2015)2290–2295.

[19] R.Anitha,P.V.Vinesh,K.C.Prakash,P.Mohanan,K.Vasudevan,ACompactQuadElementSlottedGroundWidebandAntennaforMIMOApplications,IEEETrans.AntennasPropag.64(10)(2016)4550–4553.

[20] A. Desai, M. Palandoken, J. Kulkarni, G. Byun, T.K. Nguyen,‘‘WidebandFlexible/TransparentConnected-GroundMIMOAntennasforSub-6GHz5GandWLANApplications,”inIEEE,Access9(2021)147003147015,https://doi.org/10.1109/

[21] ACCESS.2021.3123366.

[22] M.Usman,E.Kobal,J.Nasir,Y.Zhu,C.Yu,A.Zhu,CompactSIWFedDual-PortSingleElementAnnularSlotMIMOAntenna for 5G mmWave Applications, IEEE Access 9 (2021)91995–92002.

[23] W. Ali, S. Das, H. Medkour, S. Lakrit, Planar dual-band 27/39GHzmillimeter-waveMIMOantennafor5Gapplications,MicrosystTechnol27(1)(2021)283–292,https://doi.org/10.1007/s00542-020-04951-1.

[24] Z. Wani, M.P. Abegaonkar, S.K. Koul, A 28-GHz antenna for5GMIMOapplications,ProgressInElectromagnetics ResearchLetters78(2018)73–79.

[25] M.M. Kamal, S. Yang, X.-C. Ren, A. Altaf, S.H. Kiani, M.R.Anjum,A.Iqbal,M.Asif,S.I.Saeed,InfinityShell ShapedMIMOAntennaArrayformm-Wave5G Applications,Electronics10(2)(2021)165,https://doi.org/10.3390/electronics10020165.

[26] Raheel,Kiran,AhsanAltaf,ArbabWaheed,SaadHassan Kiani, Daniyal Ali Sehrai, Faisel Tubbal, and Raad Raad. ‘‘E-shapedH-slotteddualbandmmwaveantennafor5Gtechnology.”Electronics10,no.9(2021):1019.

[27] A.Desai,C.D.Bui,J.Patel,T.Upadhyaya,G.Byun,T.K.

[28] Nguyen,CompactWidebandFourElementOpticallyTransparent MIMO Antenna for mm-Wave 5G Applications,IEEEAccess8(2020)194206–194217.

[29] Khalid,Mahnoor,SyedaIffatNaqvi,Niamat Hussain,MuhibUr Rahman, Seyed Sajad Mirjavadi, Muhammad JamilKhan, and Yasar Amin. ‘‘4-Port MIMO antenna with defectedgroundstructurefor5Gmillimeterwaveapplications.” Electronics9,no.1(2020):71.

[30] Rahman,Saifur,Xin-chengRen,AhsanAltaf,MuhammadIrfan,MujeebAbdullah,FazalMuhammad,MuhammadRizwan Anjum, Salim Nasar Faraj Mursal, and Fahad SalemAlKahtani.‘‘NatureinspiredMIMOantennasystemforfuture

[31] mmWavetechnologies.”Micromachines11,no.12(2020):1083.

[32] Jilani, S.F.and Alomainy, A.,2018. Millimeter-wave T-shaped

[33] MIMO antenna with defected ground structures for 5G cellularnetworks. IETMicrowaves,Antennas&Propagation, 12(5),pp.672-677.IET

[34] D.Pozar,Surfacewaveeffectsformillimetrewaveprinted antennasvol.21(1983)692–695.

[35] N.A.Touhami,T.Elhamadi,M.A.Ennasar,High-gainandbroadbandSIWcavity-backedslotsantennaforX-bandapplications,Int.J.MicrowaveWirelessTechnolog.(2021)1–8.

[36] S.A. Saputro, S. Nandiwardhana, J.-Y. Chung, Estimation ofAntennaCorrelationCoefficientofN-PortLossyMIMOArray,ETRIJournal40(3)(2018)303–308.

[37] Rana, P. ., Sharma, V. ., & Kumar Gupta, P. . (2023). Lung Disease Classification using Dense Alex Net Framework with Contrast Normalisation and Five-Fold Geometric Transformation. International Journal on Recent and Innovation Trends in Computing and Communication, 11(2), 94–105. https://doi.org/10.17762/ijritcc.v11i2.6133

[38] Ólafur, J., Virtanen, M., Vries, J. de, Müller, T., & Müller, D. Data-Driven Decision Making in Engineering Management: A Machine Learning Framework. Kuwait Journal of Machine Learning, 1(1). Retrieved from http://kuwaitjournals.com/index.php/kjml/article/view/108